Low Cycle Fatigue Tests of Reinforced Concrete Columns and Joints, Built with Ribbed Reinforcement and Plain Stirrups

R.C. Borg & T. Rossetto
University College London, UK

H. Varum
University of Aveiro, Portugal

15 WCEE
LISBOA 2012

SUMMARY:
The majority of existing reinforced concrete (RC) buildings were built prior to the introduction of seismic codes. As observed in various recent earthquakes, due to their lack of structural capacity and ductility such structures are very vulnerable and have suffered considerable damage. The number of cyclic tests that have been carried out to investigate the behaviour of RC components with detailing typical of these buildings is very limited. Such tests are very relevant for seismic vulnerability assessment purposes. In this paper, a low-cycle fatigue testing campaign on RC columns and connections specifically devised to investigate various physical parameters that affect damage development, is presented. The campaign consists of 19 columns and 7 beam-column connections. Some of the preliminary results and observations are presented and discussed.

Keywords: Low cycle fatigue tests, RC beam-column connections, RC columns

1. INTRODUCTION

The majority of existing reinforced concrete (RC) buildings were built prior to the introduction of seismic codes. As observed in various recent earthquakes (e.g. EEFIT, 2009), due to their lack of structural capacity and ductility such structures are very vulnerable and have suffered considerable damage. The lack of structural capacity and ductility can be mainly attributed to inadequate detailing, and low strength of the constituting materials. A RC component is made up of a composite material consisting in longitudinal steel reinforcement, transverse steel reinforcement and concrete. The mechanical interaction of these three constitutes the robustness of the component. Detailing aspects such lap-splices, reinforcement anchorage, spacing of transverse reinforcement and end-anchorage of transverse reinforcement are, amongst others, responsible for the behaviour of this mechanical interaction and hence influence the performance of the RC component. Constitutive models of materials and their associated physical properties are hysteretic in nature. As a result, the behaviour of a component under earthquake loading is different from that under a monotonic load such as the component self-weight. This is due to the cyclic nature of the former (Fardis, 2009). A seismic load induces fast deformation rates, resulting in elevated stress capacity values of the individual materials (Penelis et al., 1997). Nevertheless, the cyclic nature of the seismic load induces a fatigue demand for which a RC component has a lower capacity, compared to when the same load is applied monotonically at the same strain rate level (Penelis et al., 1997).

Apart from the geometry of the detailing aspects, the type of reinforcement used has an influence on the failure modes of RC elements. Structures built prior to the 1970's were constructed with plain bars. Such structures were observed to fail ultimately by shear, bond-slip, buckling, opening of stirrups, crushing of concrete and rupture of reinforcement (EERI, 1999). Plain reinforcing bars have a lower bond strength capacity with concrete than ribbed bars (CEB, 1996; Fardis, 2009). As a result, bond-slip failure mechanism is a dominant mode in such structures and influences the development of subsequent modes of failure. On the introduction of ribbed-reinforcement, the bond mechanism was enhanced and failure modes were dominated by inadequate transverse reinforcement detailing, strength of materials and longitudinal reinforcement ratios, leading to shear, reinforcement buckling, and reaching ultimate strengths of materials, amongst others. Some practices in various countries,

continued to use plain bars for transverse reinforcement for an elongated period. Since plain bars are softer, it was easier to produce stirrups. It was only after the introduction of seismic design practices in the late 1970's, which provided adequate detailing requirements for transverse reinforcement, longitudinal reinforcement and material strength, that the vulnerability was controlled to capacity levels of the components and plasticity levels of the materials.

No consensus exists on which engineering demand parameters (EDP) and damage indices (DI) are best for the quantification of damage in RC structures pre-dating seismic codes (Borg et al., 2010). This is partly due to the insufficient experimental data available on RC components with aseismic detailing available. As part of a research trying to enhance the quantification of damage through EDPs, an experimental campaign of low-cycle fatigue tests on 19 RC columns and 7 beam-column joints was conducted. This paper provides a description of this experimental campaign and discusses some of the preliminary results.

2. THE EXPERIMENTAL TESTING CAMPAIGN

2.1 Type of Test and the Test Set-up

There are various test configurations that can be used to investigate the mechanical behaviour of RC elements under low-cycle fatigue loading. For column elements, some test-setups consider the full element (Figure 1a,b - Lee et al., 2003). In this test setup P-delta effects are considered, and the point of contra-flexure can vary along the shear span of the structure. Nevertheless, the reaction frame is required to be stiff, and a large number of actuators are needed to keep the upper and lower base-frames parallel. Another arrangement consists in 2 cantilevers spanning from a stiff foundation with the load applied at the foundation (Figure 1c). This arrangement can account for P-Delta effects. Nevertheless, the 2 cantilevers will not follow a realistic shape of deformation simultaneously. Another type of configuration consists in a cantilever representing half the length of the element (Figure 1d). The point of contraflexure is assumed to be fixed at mid-height of the length of the element. The incorporation of P-Delta effects depends on the method of application of the vertical load representing axial loading conditions. The effective force may be interpreted as a combination of lateral force and P-delta effects.

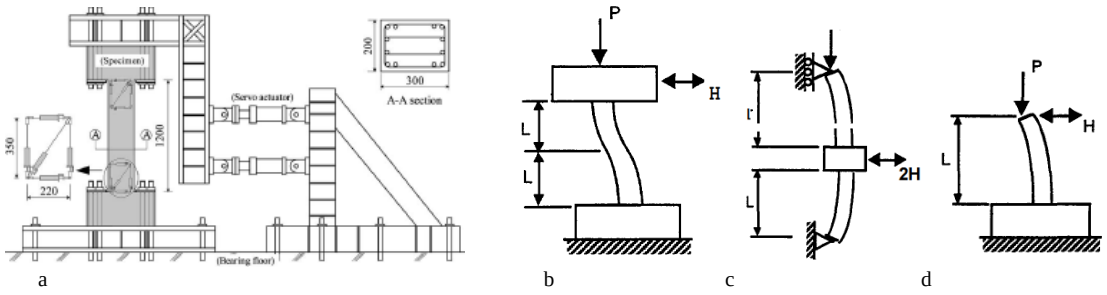

Figure 1. Different testing configurations for low cycle fatigue tests.

The experiments were carried out in the structural lab of the Civil Engineering Department at the University of Aveiro. For the column elements, the test setup adopted was based on the concept shown in Figure 1d. The RC column model consists in a cantilever representing half the depth of a storey. The setup is in the horizontal plane (Figure 2a), where the foundation is fixed by two metallic frames, and the lateral load is applied at the top of the cantilever by a hydraulic actuator in displacement control mode. The axial load is applied parallel to the axis of the element and on the upper tip of the column by a static hydraulic actuator. The axial load system is hyperstatic and excludes P-delta effects. For the beam-column joints a similar system is adopted (Figure 2b and 2c) and is based on the setup of Fernandes et al. (2011). The beams are restricted not to move in the direction parallel to the columns. The lower end of the lower column is allowed to rotate freely. Since the setup is in the horizontal plane, the gravity loads on the beams could not be simulated. For these setups (Figure 2) and for this investigation, the vertical loads were assumed to remain constant throughout the test.

Altough earthquake loading is multidirectional, uni-directional loading was considered for these tests. Since, low-cycle fatigue cyclic tests induce strains at very slow rates, it was not possible to simulate the behaviour associated to high strain rate effects that are induced by earthquakes.

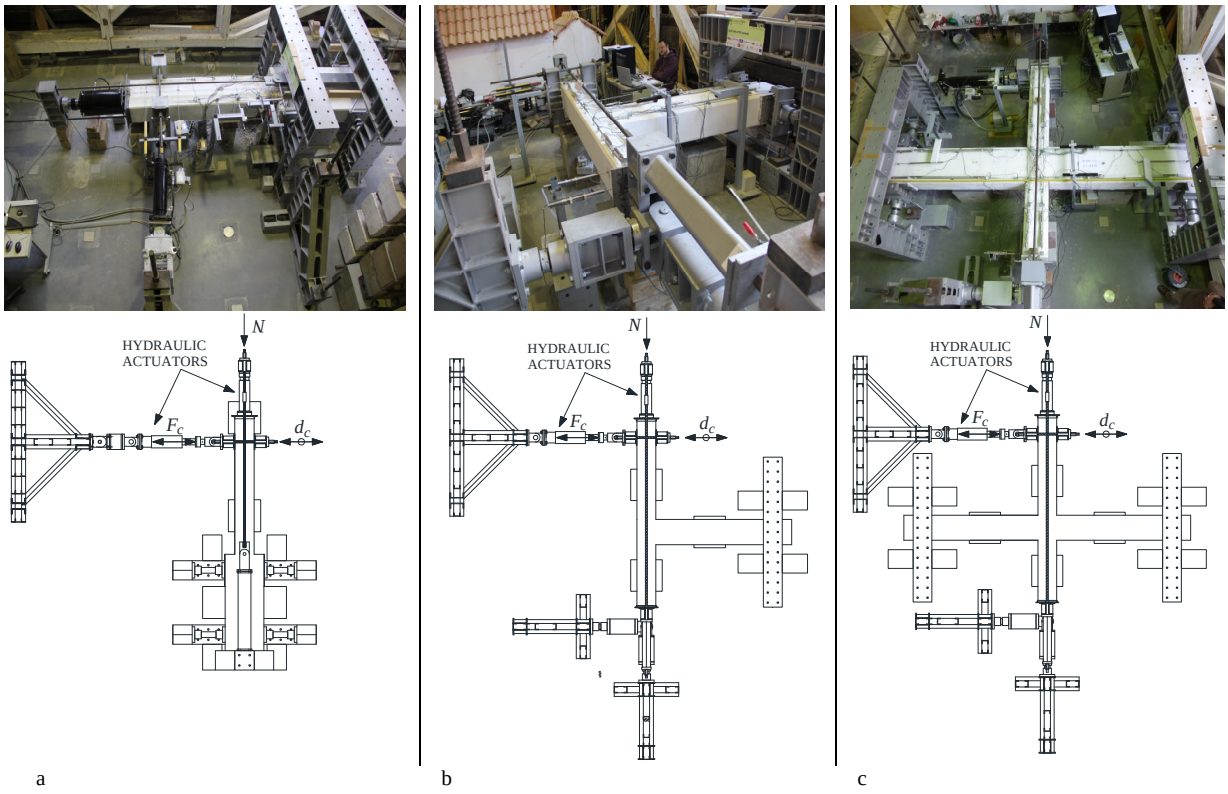

Figure 2. Test setup for: (a) column elements, (b) beam-column T-joints, (c) beam-column X-joints.

2.2 Reference Structure

The structural components that are used in the testing campaign are based on two reference RC frame structures with geometry as shown in Figure 3. The first frame was designed according to common requirements of DM 26/03/80 and BS8110 (1987). Detailing to provide structural robustness to resist earthquake loading was not provided. This RC frame geometry and design is chosen as it features in various countries across Europe. The other frame is instead seismically designed according to EN 1998-1 (2004), following the design procedure and detailing requirements suggested by Fardis (2009). For the latter case, rock ground conditions were assumed, and the structure was designed to a Peak Ground Acceleration (PGA) of 0.25g.

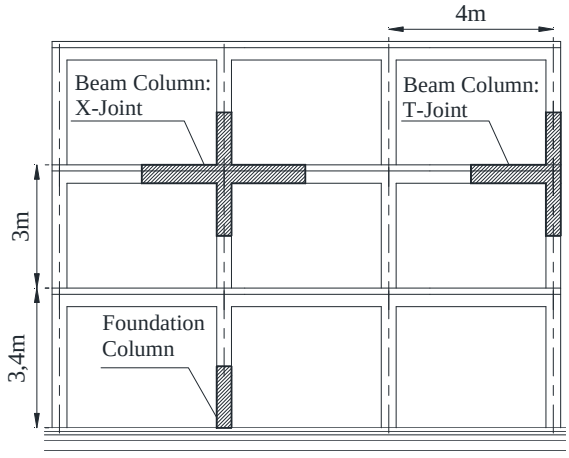

Figure 3. Reference RC frame structure.

The structure consists in a 3x3 bay structure with the lower level being slightly higher than the other levels as shown in Figure 3. The figure also indicates the parts of the frame that were considered as representative components of columns, and of internal and external beam-column joints. The points of contra-flexure are assumed to occur invariably in the middle of each element.

2.3 Scheme of Experiments: Columns

2.3.1. Detailing aspects and physical parameters of column specimens

The experimental campaign consists of 19 full scale specimens, representing any column at the base of the reference structure (Figure 3). Table 1 and Figure 4 indicate the variation of the geometry, reinforcement detailing and physical parameters for each specimen. Specimen T14 is the reference column corresponding to the first design option of the reference non-seismically designed frame. Specimen T12 is the reference column corresponding to the second reference frame designed according to EN1998-1 (2004). The cross section of both columns measures 300x300mm. Detailing aspects that distinguish T14 from T12 were varied gradually and in turn, in T1c, T2, T3, T15, T9 and T11. In T1c, 135^0 hooks are considered for transverse reinforcement instead of 90^0 hooks as in T14. In T2, additional transverse legs are incorporated, restraining all longitudinal reinforcement. In T3, the spacing of the stirrups is further reduced in order to have confinement equal to T12. In specimen T9 the percentage reinforcement is increased to correspond with that of T12. Two reinforcement ratios are therefore considered in the tests; 1% and 2.7%. The former is below the minimum required by EN1998-1 (2004).

Table 1. Scheme of the variation of parameters for tests on columns.

Element Type	Section	Concrete Grade	Load Ratio	Confinement	Reinforcement Ratio	Lateral Load pattern	Anchorage Detail	Aspect ratio of Element	Test
Column	Square: 300x300	C16/20	v=0.26	a=0.1	Reinf.=1%	LP 1	Continuous	L/h=5.7	**T14**
				a=0.1	Reinf.=1%	LP 1	Continuous	L/h=5.7	**T6**
				a=0.1	Reinf.=1%	LP 1	Continuous	L/h=5.7	**T1-c**
				a=0.22	Reinf.=1%	LP 1	Continuous	L/h=5.7	**T2**
				a=0.44	Reinf.=1%	LP 1	Continuous	L/h=5.7	**T3**
	Rectangle:300x500	C16/20	v=0.26	a=0.1	Reinf.=1%	LP 1	Continuous	L/h=3.4	**T5**
				a=0.22	Reinf.=1%	LP 1	Continuous	L/h=3.4	**T8**
	Square: 300x300	C16/20	v=0.44	a=0.1	Reinf.=1%	LP 1	Continuous	L/h=5.7	**T15**
				a=0.22	Reinf.=1%	LP 1	Continuous	L/h=5.7	**T7**
	Square: 300x300	C16/20	v=0.26	a=0.22	Reinf.= 2.7%	LP 1	Continuous	L/h=5.7	**T9**
					Reinf.= 2.7%	LP 1	Continuous	L/h=5.7	**T10**
	Square: 300x300	C16/20	v=0.26	a=0.44	Reinf.= 2.7%	LP 1	Continuous	L/h=5.7	**T11**
		C30/37	v=0.26	a=0.44	Reinf.= 2.7%	LP 1	Continuous	L/h=5.7	**T12**
	Square: 300x300	C16/20	v=0.26	a=0.1	Reinf. =1%	LP 2	Continuous	L/h=5.7	**T13**
					Reinf. =1%	LP 3	Continuous	L/h=5.7	**T1-a**
					Reinf. =1%	LP 4	Continuous	L/h=5.7	**T1-b**
	Rectangle:300x500	C16/20	v=0.158	a=0.22	Reinf.=1%	LP 5	Continuous	L/h=3.4	**T4**
	Square: 300x300	C16/20	v=0.26	a=0.1	Reinf. =1%	LP 1	LS: 35 x D	L/h=5.7	**T16-D1**
							LS: 75 x D	L/h=5.7	**T17-D2**

Three confinement ratio variations are considered as shown in Table 1. These are computed according to Fardis (2009). Specimens T5 and T8 have a different cross-sectional geometry. The normalised parameters corresponding to T14 and T2 respectively are conserved, with the exception of the span-to-

depth ratio. T15 and T7 are included to investigate the effect of varying the axial load ratio with respect to T14 and T2. Specimen T16-D1 incorporates lap-splicing equal to 35x diameter of the longitudinal reinforcement. This corresponds to the requirements of various European codes such as DM 26/03/80, before seismic detailing considerations were introduced. Specimen T17-D2 incorporates lap-splicing equal to 75xdiameter. This is above the minimum requirements according to Fardis (2009). Specimen T6 was constructed in 2 phases. In the first phase, the foundation was cast. This was allowed to cure, and the column was cast at a later stage, allowing the formation of a cold joint between the column and the foundation. This is very common in practice. Moreover, the lower part of the column was rod compacted and the concrete was allowed to bleed. The latter was also a very common construction practice, particularly in various regions of the Mediterranean which lacked adequate quality control (EERI, 1999).

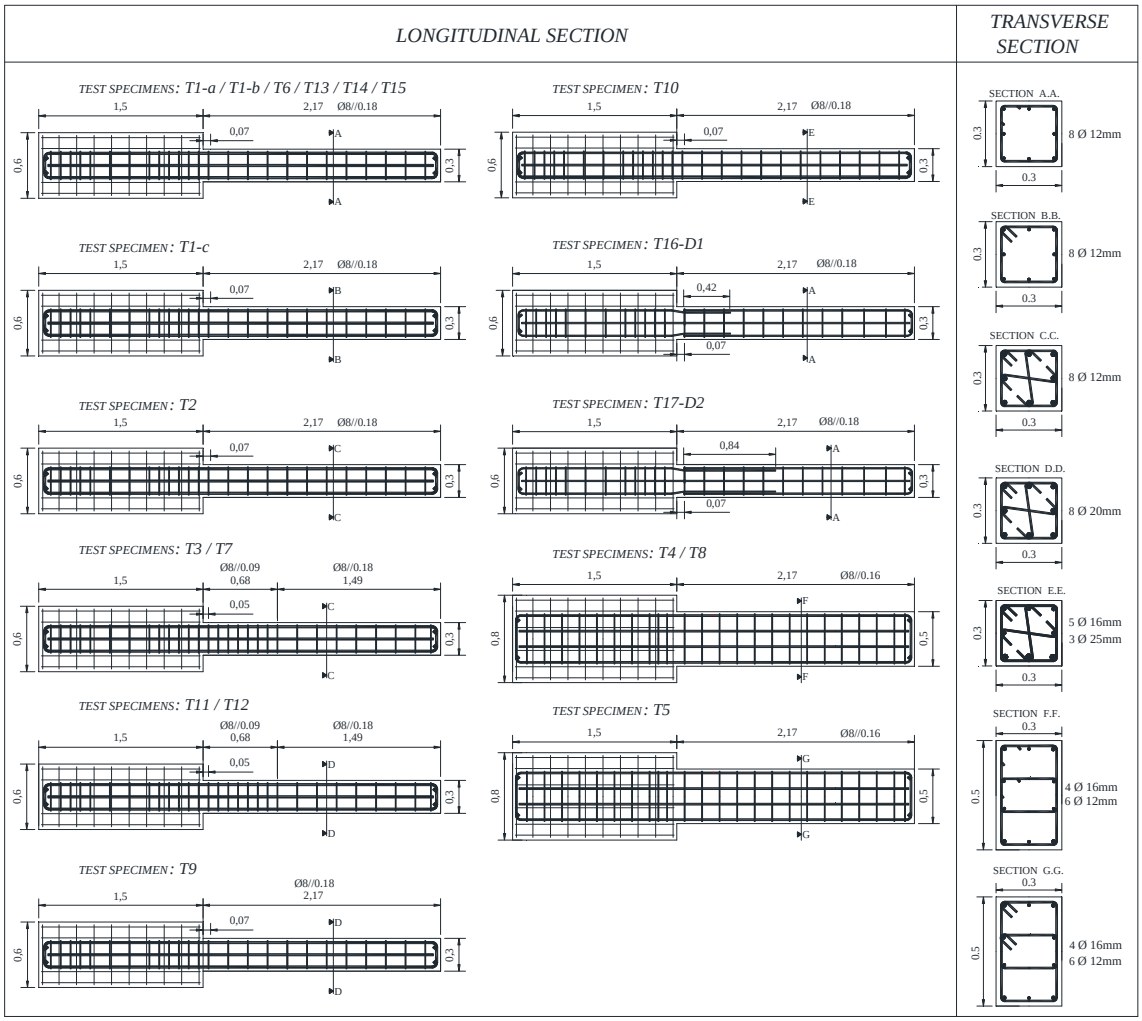

Figure 4. Longitudinal and transverse sections showing the detailing and geometry of the column specimens.

2.3.2. Cyclic loading patterns

Unlike in shaking-table experiments, the input cyclic load by the actuator in low cycle fatigue tests is equal to the response load. As a result, the expected behaviour of the component and its damage development is a function of the number of cycles and the cyclic pattern of the input loading. For specimens T13, T1a, T1b and T4, various load patterns are considered as shown in Table 1 and Figure 5. This was done in order to investigate the effect of the number of loading cycles on the behaviour of the RC elements. Load pattern LP 1 was assumed as the reference load pattern and was adopted for all the other test specimens. Further details on the development of the loading patterns and their effect on the behaviour of the structural elements can be found in Borg et al. (2012).

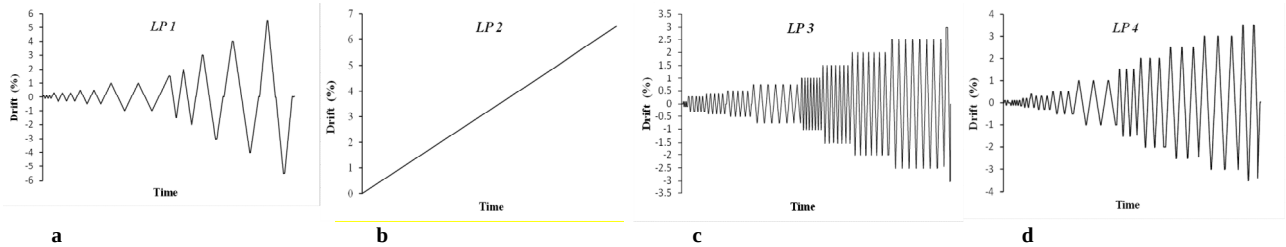

Figure 5. Displacement loading history patterns adopted in the low-cycle fatigue testing campaign.

2.3.3. Material properties

Table 2 indicates the average strength of the materials adopted in the test specimens. Tensile tests on reinforcement were performed according to EN ISO 6892-1 (2009). Concrete compression and Brazilian tests were performed on 150x300mm cylinders according to EN 12390-3 (2009). The average compressive strength for most specimens was found to be 19MPa. Only specimen T12 was constructed with a higher strength of concrete. This was done in order to meet the minimum requirements of EN1998-1 (2004). The average compression strength for this specimen was found to be 37MPa. The average tensile strength of the specimen based on the Brazilian test was found to be 2.2MPa. Since, the tests were conducted in Portugal, the material properties were influenced by products available locally. Nevertheless, the values indicated in the table show that these also represent materials found in other European regions (Fardis, 2009). The 8mm Ø plain bars used as transverse reinforcement have a very low strength. This corresponds to mild-steel that was very common before the introduction of seismic codes. The low value of yield strength of the 12mm Ø ribbed bars is typical of high-strength steel before the introduction of seismic codes, particularly where quality control of materials was not strict.

Table 2. Properties of steel and concrete materials based on average values.

Concrete		Steel Reinforcement														
		Plain (A235)			Ribbed (A400NRSD)											
		8mm Ø			8mm Ø			12mm Ø			16mm Ø			20mm Ø		
f_{cm} (MPa)	f_{ct} (MPa)	f_{yk} (MPa)	f_{uk} (MPa)	f_{uk} / f_{yk}	f_{yk} (MPa)	f_{uk} (MPa)	f_{uk} / f_{yk}	f_{yk} (MPa)	f_{uk} (MPa)	f_{uk} / f_{yk}	f_{yk} (MPa)	f_{uk} (MPa)	f_{uk} / f_{yk}	f_{yk} (MPa)	f_{uk} (MPa)	f_{uk} / f_{yk}
19	2.0	360	450	1.25	470	569	1.21	416	548	1.32	470	580	1.23	470	585	1.24

2.4 Scheme of Experiments: Beam-Column Connections

The experimental campaign of the beam-column (b-c) connections consisted in 7 specimens, of which 2 were T-joints, representing the exterior column and beam of the frame, and 5 were X-joints, representing an internal column connected with beams on either side of the node panel. Table 3 indicates the schematic variation of the physical properties of each test specimen. Figure 6 shows the geometry and the detailing aspects of the beam-column connections. All the b-c connections were constructed without slab flanges, with the exception of J4-X where the effective length was based on the requirements of EN1998-1 (2004). A slab depth of 15mm was considered. For all specimens, the cross section of the beams was taken as 300x500mm, whereas for the columns this was taken as 300x300mm. On conducting a moment-curvature analysis at section level for the beam and the general column, the moment capacity of the former was found to be 130kNm, while the moment capacity of the column was found to be 47kNm. This is a typical strong-beam weak-column situation which characterised soft-storey failure mechanisms in past earthquakes (EERI, 1999).

The confinement in the beams was kept constant for all specimens, while the confinement in the column was only varied for J7-X. The confinement in the joint was introduced in J5-X and J7-X. Joint confinement was not a popular practice before the introduction and adoption of seismic codes. Nevertheless, this was incorporated in these specimens in order to investigate how the behaviour of the system evolves on such inclusion. Lap-splice effects were investigated in exterior b-c connection J2-T

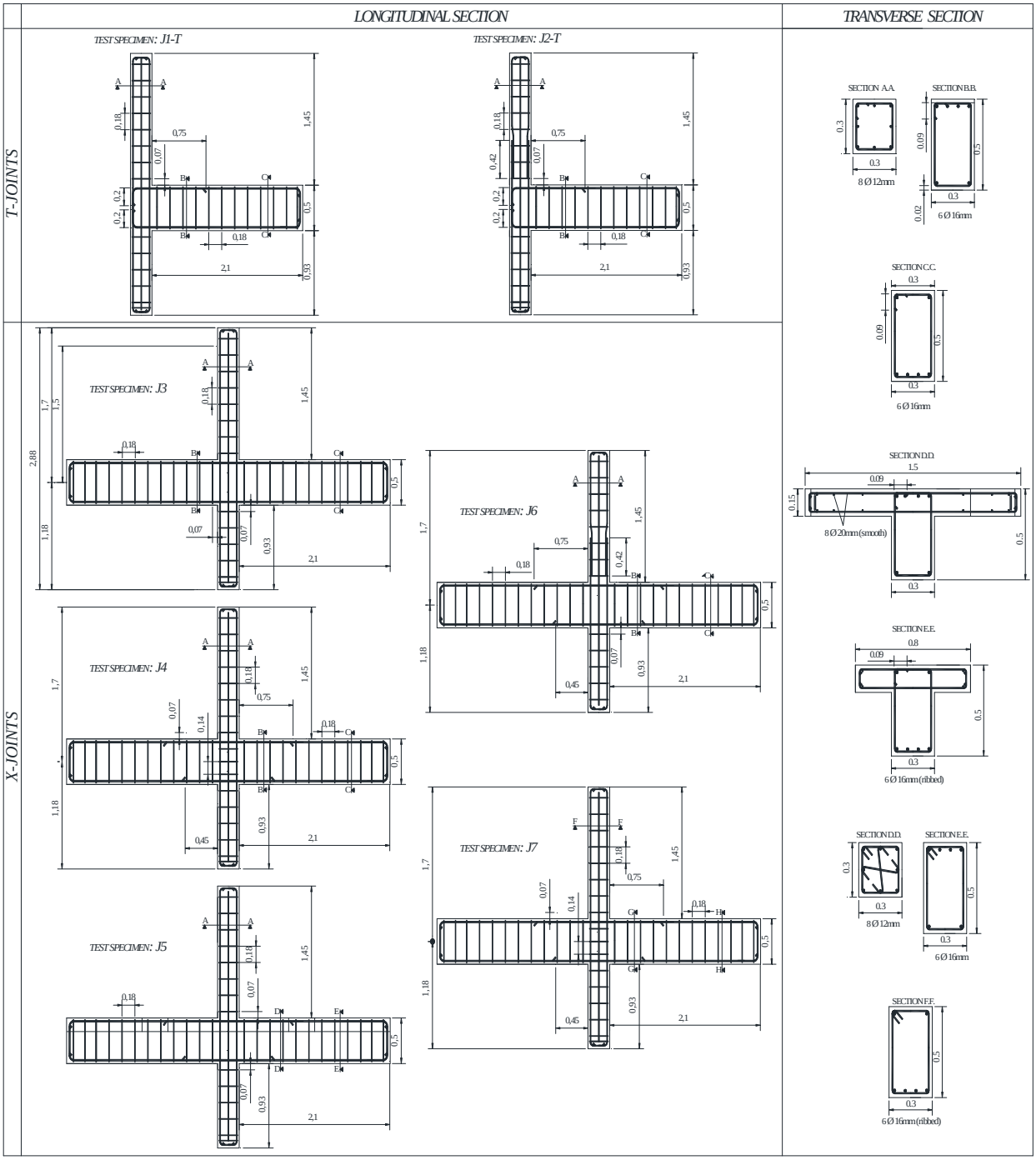

Figure 6. Longitudinal and transverse sections showing the detailing and geometry.

Table 3. Scheme of the variation of parameters for tests on beam-column joints.

Element Type	Section	Concrete	Load Ratio	Confinement	Reinforcement Ratio	Lateral Load pattern	Anchorage Detail	Aspect ratio of Element	Test
Inner T-Joint	Square: 300x300	C16/20	v=0.26	a=0.1	Reinf. =1%	LP 1	Continuous	L/h=5	**J1-T**
							LS: 35 x D	L/h=5	**J2-T**
Inner X-Joint	Square: 300x300	C16/20	v=0.26	a=0.1	Reinf. =1%	LP 1	Continuous	L/h=5	**J3-X**
							Conf. Node	L/h=5	**J5-X**
							Continuous	L/h=5	**J4-X**
							LS: 35 x D	L/h=5	**J6-X**
	Square: 300x300	C16/20	v=0.26	a=0.22	Reinf. =1%	LP 1	Conf. Node	L/h=5	**J7-X**

and interior b-c connection J6-X. In both cases the lap-splice length was considered to be equal to 35x the bar diameter. Although gravity loads on beams could not be incorporated, curtailment of reinforcement was still provided for all specimens, with the exception of J3-X where symmetric reinforcement was provided. The strength of materials and loading pattern are similar to those adopted for the column specimen campaign.

3. PRELIMINARY RESULTS OF THE LOW-CYCLIC FATIGUE TESTS

The results, observations and comparisons produced and discussed here are based on general observations and the resulting force-drift capacity of the structural elements. In general, cracking was observed to start at 0.3% drift for columns and 0.1% for beam-column connections. The main modes of failure consisted in crushing of concrete, buckling of the main reinforcement, rupture of the main reinforcement, opening of stirrups, and bond-slip mechanism (mainly when lap-splice or reinforcement anchorage was investigated). The comments and observations made refer only to the specific and particular cases discussed, and may not necessarily apply to other particular situations.

3.1 Column Specimens

Since most physical parameters and detailing aspects of the tested specimens are variants to corresponding parameters of specimens T14 or T12 as previously discussed, most comparisons will be made with these two specimens. Figure 7a and 7b indicate that both the 300x300mm section and the 300x500mm section incorporating 135^o hooks in the transverse reinforcement, have a slightly increase in the maximum force capacity over corresponding sections with 90^o hooks. Having 90^o hooks, T5 failed at 4% drift through the opening of the transverse reinforcement hoops. This was not the case for T8, where the 135^o hook remained embedded in the concrete, and the element collapsed at 4.5% drift. Figure 7c confirms that ductility increases with an increase in confinement. Nevertheless, an increase in strength is observed when all the bars are restrained. Figure 7d, shows that ductility increases with lap-splicing. This arises since the region over which buckling is observed in T14, is now resisted by the dual action of the overlapping bars. Figures 7e and 7f show the increase in ductility with increase in confinement and total reinforcement ratio. However, Figure 7g shows that the increase in confinement does not affect the maximum strength. Figure 7h indicates that for the same load ratio, reinforcement ratio and confinement ratio, the strength decreases and the ductility increases with the aspect ratio. On increasing the load ratio, the initial stiffness and strength of the component increases. Nevertheless, since the axial load ratio is close to the maximum capacity of the column, the component does not exhibit ductility, (see Figure 7i).

3.2 Beam-Column Connections

Joint J1-T is the reference specimen for the two T-connections, whereas J3-X is the reference specimen of the X-connections. As shown in Figures 8a and 8d, the T-connections and the X-connections without lap-splices reach a higher maximum strength when compared to the corresponding b-c connections with lap-splices. As previously discussed, the columns with lap-splice exhibited the same maximum stress as the corresponding specimen without lap-splice. In the case of the columns, both the foundation and the column are very stiff. In the case of the joints, the column is considered stiffer than the joint particularly since the latter is not confined. As a result, for a particular drift, more deformation is absorbed by the joint and the maximum capacity of the continuous reinforcement section is not reached in the lap-spliced specimen. Nevertheless, in Figure 8d it is observed that the lap-spliced specimen T6-X has a higher ductility than T3-X, as the former delays the formation of buckling due to the dual action of the lapped reinforcement in the upper column part of the b-c connection. Figures 8b and 8c show that the edge columns have a lower strength and ductility capacity than the interior columns. The maximum shear force attributed to the external columns is generally lower than that in the internal columns. As a result, a lower strength capacity in the external joints may not necessarily be a problem. Nevertheless, since the drift demand in an earthquake is generally the same for all columns within a particular level, a lower ductile capacity may result in a possible soft-storey failure. Specimen J5-X in Figure 8f shows how confinement in the joint induces

larger ductility capacities. However, if this confinement results in a stiffer beam compared to its corresponding intersecting columns, the ductility decreases and a sudden collapse mechanism may be expected, as is observed in specimen J7-X. In Figure 8e, specimen J4-X shows that the incorporation of the slab increases the stiffness of the beam and the joint in relation to the stiffness of the column, resulting in a reduction in the system ductility. More damage is observed to form in the columns, whereas damage formed in the beams propagates also in the slab.

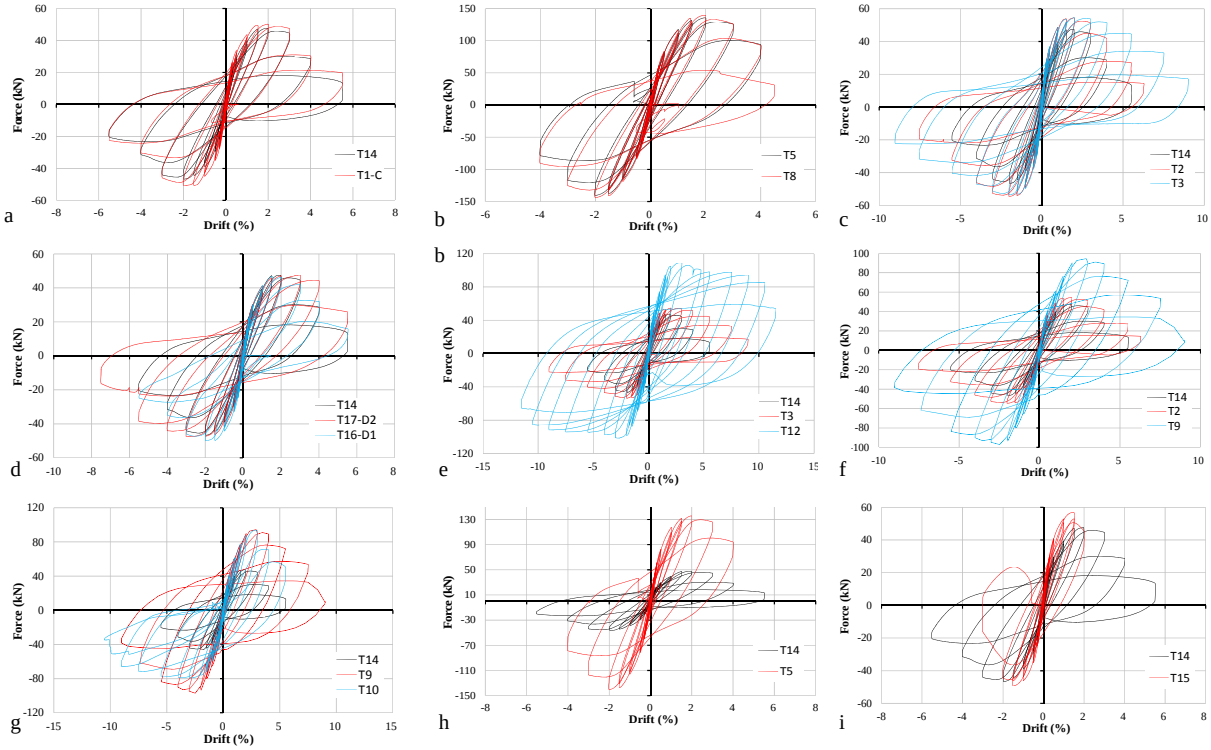

Figure 7. Comparison of the capacity of the column specimens in terms of the force-displacement relation.

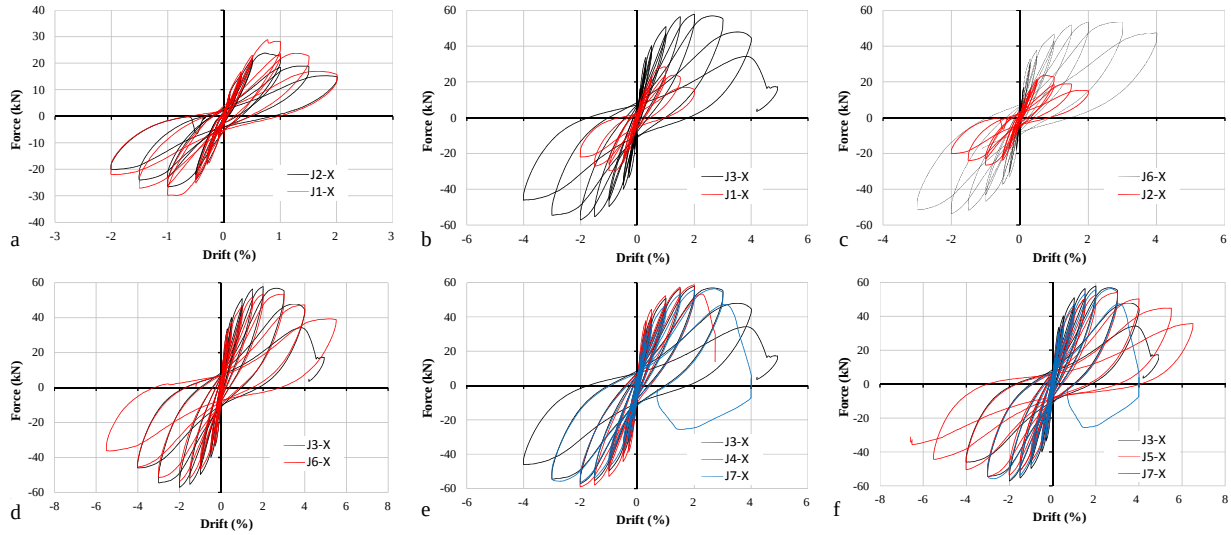

Figure 8. Comparison of the capacity of the beam-column joint specimens in terms of force-displacement.

4. CONCLUSIONS AND FURTHER RESEARCH

A testing campaign of RC columns and beam-column connections was carried out with the aim to investigate the vulnerability of structural components that are not adequately designed to resist earthquakes. Within the testing campaign detailing parameters were varied to investigate their effects on the overall cyclic behaviour of the columns and connections. The preliminary observations indicate that an increase in confinement in columns can contribute to an increase in column ductility, as expected, whereas the excess of confinement in joints can contribute to a reduction in the ductility of beam-column connections. If adequate bond is provided in lap-splices, these can contribute to the prevention of buckling. The incorporation of the slab in beam-column connection specimens was observed to have a large influence on the behaviour of the connection. The observations and results presented here are only preliminary and are based on force-displacement response of the components. The behaviour of the tested specimens is now also being interpreted and quantified in terms of energy dissipation, type of damage development, damping, strength degradation and stiffness degradation. Since damage development is a cumulative process, this will give a better understanding of the quantification of damage in terms of engineering demand parameters at intermediate levels of damage.

ACKNOWLEDGEMENTS

The authors would like to thank the Department of Civil Engineering at the University of Aveiro for allowing the experiments to be carried out in its laboratories and for their practical technical support. The research is financially supported by EPSRC (UK) and by the Strategic Educational Pathways Scholarship (Malta). The latter is part-financed by the European Union – European Social Fund (ESF) under Operational Programme II – Cohesion Policy 2007-2013, "Empowering People for More Jobs and a Better Quality of Life".

REFERENCES

Borg, R.C. and Rossetto, T. (2010). Comparison of Seismic Damage Indices for Reinfroced Concrete Structures. *14th European Conference on Earthquake Engineering*, Ohrid, F.Y.R.O. Macedonia.

Borg, R.C. Rossetto, T. and Varum, H. (2012). The effect of the number of response cycles on the behviour of R.C. elements subject to cyclic loading. *15th World Conference on Earthquake Engineering*, Lisbon, Portugal.

BS8110:Part1 (1985). Structural use of concrete. Part 1. Code of practice for design and construction. British Standard Institution.

CEB (1993). Bond and Detailing: Selected Justification Notes. CEB Report No. 217.

EEFIT (2009). The L'Aquila, Italy Earthquake of 6 April 2009: A Preliminary field report, Earthquake Engineering Field Investigation Team (EEFIT).

EERI (1999). Structural Engineering Reconnaissance of the August 17, 1999 earthquake: Kocaeli (Izmit), Turkey. PEER Report 2000/09.

EN12390-3 (2009). Testing Hardened Concrete-Part3: Compressive strength of test specimens. European Committee for Standardization (CEN).

EN1998-1(2004). Eurocode 8: Design of structures for earthquake resistance – Part1: General rules, seismic actions and rules for buildings. European Committee for Standardization (CEN).

EN ISO 6892-1 (2009). Metallic materials – Tensile testing Part 1: method of test at ambient temperature. Committee for Standardization (CEN).

Fardis, M. (2009). Seismic design, assessment and retrofiting of concrete buildings. Springer.

Fernandes (2011). Comparative analysis of the cyclic behaviour of beam-column joints with plain and deformed reinforcing bars. *IBRACON Structures and Materials Journal*. **4-1**: 147-172.

Penelis, G. and Kappos, A. (1997). Earthquake-Resistant Concrete Structures. Francis and Taylor, London, UK.

Lee, J.Y. and Watanabe, F. (2009). Prediciting the longitudinal axial strain in the plastic hinge regions of reinforced concrete beams subject to reversed cyclic loading. *Engineering Structures.* **25**: 927-939.

UBC (1979). Uniform Building Code. International Conference of Building Officials, California, USA.